British Journal of Applied Science & Technology
8(2): 180-193, 2015, Article no.BJAST.2015.196
ISSN: 2231-0843

SCIENCEDOMAIN *international*
www.sciencedomain.org

Synthesis, Characterization and *In vitro* Cytotoxicity Assessment of Eggshell-derived β-$CaSiO_3$ Nano Biomaterial

Boniface Tiimob[1], Vitus Apalangya[1], Tsemesgen Samuel[2], Shaik Jeelani[1] and Vijaya Rangari[1*]

[1]Department of Materials Science and Engineering, College of Engineering, Tuskegee University, Tuskegee Alabama, 36088, USA.
[2]Departments of Pathobiology, College of Veterinary Medicine and Allied Health Sciences, Tuskegee University, Tuskegee Alabama, 36088, USA.

Authors' contributions

This work was carried out in collaboration between all authors. Authors BT, VR and TS designed the study. Author BT managed literature search, wrote the protocol and first draft of the manuscript. Authors BT and VA managed the analyses of the study. All authors read and approved the final manuscript.

Article Information

DOI: 10.9734/BJAST/2015/16811
Editor(s):
(1) Wen Shyang Chow, School of Materials and Mineral Resources Engineering, Engineering Campus, Universiti Sains Malaysia, Malaysia.
Reviewers:
(1) Anonymous, Poland.
(2) Peter Anca, Department of Chemistry, Technical University of Cluj Napoca, Romania.
Complete Peer review History: http://www.sciencedomain.org/review-history.php?iid=1070&id=5&aid=8601

Original Research Article

Received 14th February 2015
Accepted 12th March 2015
Published 27th March 2015

ABSTRACT

This study explored the conversion of bio waste into a valued bioceramic material for potential tissue regeneration application. Calcium silicate (β-$CaSiO_3$) nanomaterial was synthesized from waste egg shells ($CaCO_3$) and silica (SiO_2) precursors using noninvasive but sustainable and industrially scalable ball mill and sonochemical techniques. The development of the β-$CaSiO_3$ NPs was monitored with Fourier transform infra-red spectroscopy (FTIR), thermogravimetric analysis (TGA), transmission electron microscope (TEM), field emission scanning electron microscopy / energy dispersive spectroscopy (FESEM-EDS) and X-ray diffraction (XRD). The results revealed the formation of polycrystalline nano-β-$CaSiO_3$ with 100% peak at 2θ° = 30.0 in the (320) crystal planeand sizes less than 50 nm. *In vitro* cytotoxicity studies on human osteoblast cell line CRL

**Corresponding author: E-mail: rangariv@mytu.tuskegee.edu;*

11372 suggests biocompatibility and non-interference with cell growth at concentrations ranging from 0.0781-1.250 mg/mLof β-$CaSiO_3$.

Keywords: Eggshell; calcite; diffraction; bioceramic; biocompatible; crystallite.

1. INTRODUCTION

One common source of natural bio-minerals is the chicken eggshell, which is mainly $CaCO_3$. In the US, millions of kilograms of eggshells are produced as waste yearly [1]. Though this immensely impacts the environment, the potential of deriving functional materials from the eggshell is great. Efforts for conversion into valuable biomaterials are limited [2]. This mismatch exists even in developed countries where increase in per capita income lead to proportionate increase in the generation of solid residues [3]. To maintain a balanced ecosystem, waste need to be effectively and sustainably managed in innovative ways, for example by turning them into resources [4] to supplement the practice of recycling and reuse [3]. Beside the impact on environment and landscape by piles of residue, the repugnant gas (H_2S) emitted by microbes decomposing the eggshell may endanger life [3]. However, this principal untapped source of $CaCO_3$ can be useful to the manufacture of many biomaterials. The eggshell contains 95% calcite crystals ($CaCO_3$) [5] which can be converted to β-$CaSiO_3$ in a more environmentally friendly way compared to artificial precursors which leave behind toxic wastes. β-$CaSiO_3$ possesses properties suitable for hard tissue repair, due to its biocompatibility, bioactivity and biodegradability [6], and facilitates damaged tissues in-growth to full integration with normal tissues [7]. Teeth root-end perforation repair, pulp-capping, occlusion of dentine tubules [8] and bonelike apatite formation are possible with β-$CaSiO_3$ [9]. Also, β-$CaSiO_3$ has shown promise in industrial uses in materials like plastics, ceramics, metals, paints, paper, friction products and for asbestos replacement [10]. The sol-gel and rock mining techniques for deriving $CaSiO_3$ are less sustainable. The sol-gel processes consume toxic chemical that leave behind excess acid wastes, nitrates and salts, even if bio-derived precursors are involved [11-13]. Whiles acids are corrosive, nitrates cause eutrophication in aquatic environments, leading to suffocation and bioaccumulation in organisms. Nitrates pollute drinking water and lead to reduced oxygen transport by hemoglobin when consumed. They are also linked to cancer of the digestive tract, bladder and ovary, birth defects, diabetes mellitus, thyroid hypertrophy, spontaneous abortions and respiratory tract infections [14]. Rock mined $CaSiO_3$ require further refinement and directly lead to the loss of natural habitats, land, water and air pollutions [15]. Hence, the focus of this work is to synthesize β-$CaSiO_3$ NPs from waste residue as an environmentally friendly alternative to the current methods. Nanomaterials have shown better cytocompatibility and superior mechanical, electrical, optical, catalytic and magnetic properties than their micron sized counterparts [16]. However, in dealing with NPs, their toxicity is a major concern, and is equally as important to determine as their desirable properties. The adverse effects to normal physiology, structure of organs and tissues and to the environment by NPs depends on factors like size, shape, surfacecharge and chemistry, composition, and theirstability [17-22]. The increased use of nanomaterials in society has made their toxicity a major concern [19]. Printer toners, varnishes, biomedical, cosmetic and food products are already using nanomaterials [17,19]. The market size for nanoscale pharmaceutical products is projected to increase by US $180 billion annually from 2010- 2015 [23]. With this upsurge in nanomaterials consumption, their toxicity issues cannot be overlooked. Theinhalation of 20 nm of TiO_2 at 10 mg/m^3 resulted in lung tumor, while 1.4 nm size of gold spheres lead to necrosis, mitochondrial damage, and oxidative stress on cell lines compared to 15 nm [18]. These observations highlight the potential size-dependent toxicity of NPs. Also, the lifespan of mice were reduced by NPs with sizes outside the range of 8-37 nm [24]. Cytotoxic effects of cadmium-based quantum dots on Caco-2 cells at 2-200 nmol/mL concentrations showed that 200 nmol/mL was toxic [25]. Though most nanomaterials are useful, much is not known about their toxic effects [19,24]. In this study bioactive β-$CaSiO_3$ NPs were synthesized through techniques that avoid toxic solvents [13] by the of use eggshell-based $CaCO_3$ and SiO_2 as precursors. Their cytotoxic effects were examined *in vitro* using human osteoblast cells.

2. MATERIALS AND METHODS

2.1 Separation of $CaCO_3$ Precursor from Eggshells

Egg shells were obtained from American dehydrated food Inc., Atlanta Georgia, USA and processed to separate the $CaCO_3$ crystals. The eggshell consists of ordered layer of calcified crystals precisely arranged on three types of collagen and glycosaminoglycans. Separation of the $CaCO_3$ requires the denaturing of these organic platforms. Hence the eggshells were boiled at 100ºC in an electric cooker (Hamilton Beach 33157) for 6 h and blended in a warring blender at high speed for 10 min. This was thoroughly washed with water in the initial stages and ethanol in the final stage before air-drying at room temperature for 24 h.

2.2 Synthesis of Calcium Silicate (β-$CaSiO_3$)

Beta-$CaSiO_3$ was synthesized from combined eggshell-source $CaCO_3$and SiO_2 (obtained from Nano structured & Amorphous materials Inc. NM, USA) by ball milling (Spex Sample Prep 8000D). A 1:1 mixture of $CaCO_3$ and SiO_2 was ball milled for 100 min in two separate canisters, each containing 5 g of the precursors and 8 pieces of 6 mm steel balls. About 8 g of the mixture was then sintered from room temperature to 1000ºC at a rate of 10ºC min^{-1} and allowed to stay for 3 h before cooling back to room temperature in a vacuum tube furnace (GLS-1300X). The product (~5 g) was crushed in a ceramic mortar and ball milled again for 10 h in 10 mL polypropylene glycol medium. It was then washed 4 times using ethanol and centrifuged at 12000 rpm for 10 min in Beckman Coulter (ALLEGRA-64R). This was then dispersed in 50 mL ethanol and ultrasonicated using Sonics vibra cell (WCX 750) at amplitude of 50%, temperature of 25ºC for 3 h, then centrifuged at 12000 rpm in Beckman Coulter (ALLEGRA-64R) before vacuum drying for 24 h.

2.3 Characterization of the Precursors and β-$CaSiO_3$

2.3.1 Fourier transforms infrared spectroscopy

Fourier transform infrared spectroscope (FTIR) for functional groups analysis of the synthesized $CaSiO_3$ was done using Shimazu (FTIR-8400S) equipped with IR Solutions software.

2.3.2 X-ray diffraction (XRD) analysis

X-Ray diffraction pattern of the precursors and the synthesized material and intermediates were determined using a Rigaku diffractometer (D-max 2100) equipped with monochromatic CuKα radiation (λ = 0.15406 nm). These tests were carried out at 40 KV and 30 mA, 5ºC min^{-1} sampling rate, 0.020 sampling width from 3ºC to 80º of 2θ degrees.

2.3.3 Thermogravimetric analysis (TGA)

Thermogravimetric analysis of the ball milled mixture was carried out to understand the transformations of the precursors to β-$CaSiO_3$, using TA Q500 instrument run at 10ºC/min from room temperature to 980ºC under N_2 gas at a flow rate of 60 mL/min.

2.3.4 Electron microscopy-energy dispersive spectroscopy

Transmission electron microscopy (TEM) analysis of the material was carried out using JOEL-2010 microscope. The sample was prepared by dispersing 1 mg powder in 5 mL of ethanol for 10 min in an ultrasonic bath. A drop was placed on a copper grid (200 meshes) for analysis. The microstructures and elemental composition of the β-$CaSiO_3$ NPs were determined using field emission scanning electron microscope/energy dispersive spectroscopy (FESEM/EDS) JEOL-7000 F operated at 10 kV.

2.4 Cell Cytotoxicity Studies

2.4.1 Preparation of β-$CaSiO_3$ stock suspensions

A stock suspension of β-$CaSiO_3$ NPs (10 mg/mL) was prepared in phosphate buffered saline (PBS). The stock was serially diluted into the desired concentrations using 9 autoclaved vials. About 608 µL of media was put into the first vial while 320 µL was put in the remaining eight. Then 32 µL of the stock was added to the first vial to make a total of 640 µL. This was vortexed and 320 µL pipetted and serially transferred from the second to the ninth vial.

2.4.2 Cell culture and attachment

Cells were grown in Dulbecco's modified eagle's media (DMEM) containing 10% fetal bovine serum (FBS) and antibiotic (100 units/mL penicillin-G, and 100 µg/mLof streptomycin) in 100 mm diameter dishes. These were incubated at 37ºC, in a humidified incubator supplied with 5% CO_2. Frozen fibroblasts (ATCC, CRL 11372) cells were thawed in warm water and transferred into the dishes containing culturing medium and incubated again under the same conditions for 24 h. The cells were removed from the incubator and 5 mL solution made of 0.25% trypsin and 0.03% ethylene diamine tetra acetic acid (EDTA) was added to detach them from the dishes. These were then transferred into a 15 mL tube and centrifuged at 900 rpm for 5 min to pellet the cells. The supernatant was replaced with 1 mL of DMEM and mixed to re-disperse the cells. Cell concentration was determined by loading a 10 µL aliquot of the cell suspension onto a counting hamber slide, and TC 10 automated cell counter (Bio-RAD, Hercules, CA) was used to count the cells. A final dilution of cells was made based on the cell count, to make a volume of 3 mL containing 1.0 x 10^5 cell/mL and used in the experiments.

2.4.3 Treatment of cell with $CaSiO_3$ suspension

Approximately 100 µL of the cell solution was pipetted out of the 3 mL (1.0 x 10^5 cells/mL) into each of 21 wells of a 96-well plate arranged in triplicates. This was incubated for 24 h to allow cells to attach to the plate surface. The medium was aspirated and 100 µL of the various serially diluted concentrations of $CaSiO_3$ NPs were added as treatments in triplicates. The first set of three wells served as negative control (only cells and media) whiles the second served as positive control (10 µL of 10 µM staurosporine and 100 µL cell each). These were again incubated for 24 h and 48 h in different well plates.

2.4.4 Cell titer-Glo viability assay

Cell viability was determined by Cell Titer-Glo assays (Promega Corp) which measured the luminous intensity of the chemical action of the enzyme luciferase on luciferin substrate. The enzymatic reaction uses Adenosine Triphosphate (ATP) provided only by living cells. This serves as a measure for the viability of treated cells. The degree of enzymatic reaction measured by light emission indicates the degree of cell viability in a well. This reaction and light generation were measured using a micro plate reader (BioTek, Winooski, VT). In each well, 100 µL of Cell Titer-Glo reagent was added and agitated in an incubator for 2 min at 30 rpm. This was removed and left at room temperature for 10 min before measuring the luminosities.

2.4.5 Optical microscopy

Optical micrographs of the control and cells treated with 100 µL of each concentration of β-$CaSiO_3$ used in the cytotoxicity assays were taken with Olympus IX -71 inverted microscope (model IX2-ILL100) equipped with Olympus SC30 camera and CellSens imaging software. The cells and treatments were incubated in sterile 60 x 15 mm well plates for 5 days. Micrographs were taken at 24 h intervals up to the fifth day to assess the cell interactions with the $CaSiO_3$ and compare with the viability results.

3. RESULTS AND DISCUSSION

3.1 Monitoring of $CaSiO_3$ Development from the Precursors

Thermogravimetric analysis (TGA) was used to monitor thermal transitions related to the reaction between the mixture of $CaCO_3$ and SiO_2 (1:1) during decomposition and subsequent formation of β-$CaSiO_3$ from the precusors and to establish the temperature range within which the reaction will spontaneously proceed. Fig. 1 shows TGA thermograms obtained during such transition with (a) percent weight lost and its (b) derivative curve. The various transitions can be seen in the derivative weight loss curve in Fig. 1b. It shows the first transition at about 100ºC which is due to absorbed moisture in the sample.

The second transition occurs at around 500ºC, due to the escape of carbon dioxide gas, thus as $CaCO_3$ is heated up to 500ºC it decomposes to calcium oxide and carbon dioxide (CaO and CO_2). A transition between 550ºC and 700ºC is as a results of the transformation of the reactants to an amorphous phase of calcium silicate. Between 700 - 800ºC a stable form of $CaSiO_3$ was formed with no noticeable change in weight as seen on the curve. Report show that optimal stabilization of β-$CaSiO_3$ occurs within this range whiles crystallization occurs afterwards [26]. The transition at 850ºC is attributed to changes from amorphous to crystalline phase. Based on this information it became apparent that $CaSiO_3$ was

obtainable if the reactants are subjected to controlled temperatures up to 1000ºC. X-ray diffraction performed on the residue after TGA analysis revealed polycrystalline diffracted peaks which matched *wollastonite*.

FTIR analysis was also performed on both the mixture and the TGA residue. This was done to determine the functional groups present in the precursors prior to the heating and those in the residue after the formation of a stable product. Fig. 2 shows FTIR spectra obtained from the mixed precursors and the residue samples. Characteristic stretching bands associated with bonds in β-$CaSiO_3$ were identified between wavenumbers 850-1000 cm^{-1}. These stretching bands observed on the sintered sample (a) are absent in the mixture of reactants in curve (b) prior to TGA analysis. The absence of these bands is an indication that no reaction occurs at this stage between the reactants during the ball milling process.

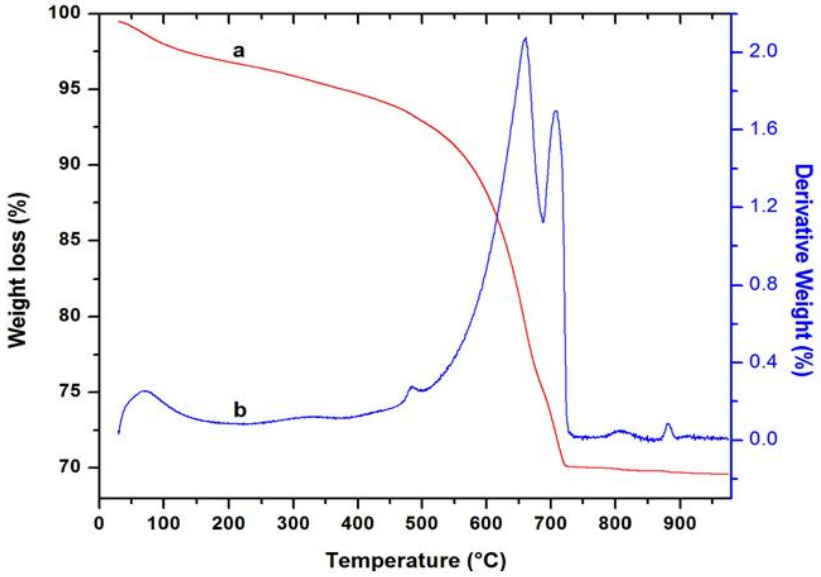

Fig. 1. TGA curves depicting the formation of β-$CaSiO_3$: a) weight loss vs temperature, b) derivative weight loss

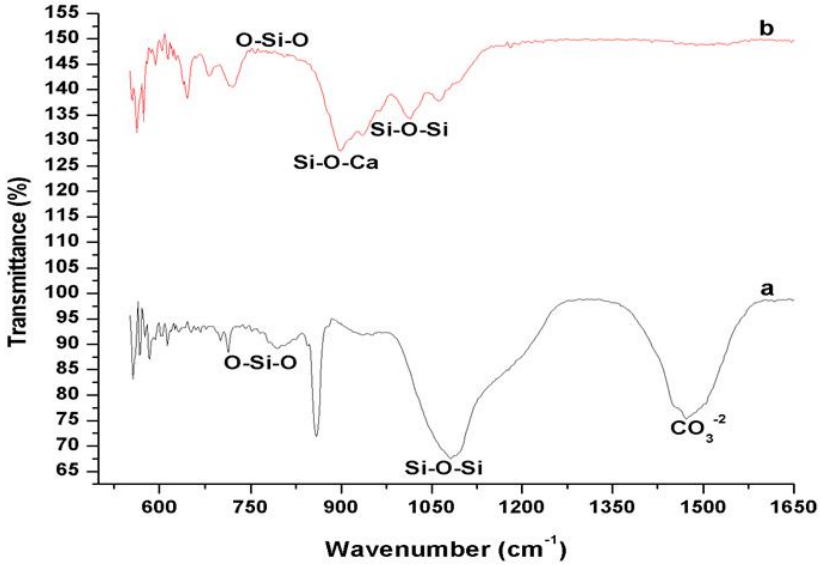

Fig. 2. FTIR Spectra: (a) $CaCO_3$ and SiO_2 mixture,(b) residue after TGA analysis

In curve (b), the stretching band between 1410-1490 cm^{-1}(asymmetric stretching vibration) and at 856 cm^{-1} (out-of-plane bending vibration) has been reported to be due to vibration of carbonate ion (CO_3^{-2}) [10,26]. This affirmed that the precursors still existed as a mixture. The broad stretch between 850 -1000 cm^{-1} is due to Si-O-Ca vibration, an indication that β-$CaSiO_3$ was formed. Similar result has been reported in a sol-gel derived β-$CaSiO_3$ from calcium nitrate and tetraetoxysilane, using water, acetic acid, ammonia and nitric acids as catalysts [27]. Symmetric stretching vibrations of Si-O-Si bonds are also observed at 1080 cm^{-1} while the stretching mode of O-Si-O featuresat 800 cm^{-1} [28].

3.2 X-ray Characterization of $CaCO_3$ (egg shell) and SiO_2 Precursors

The membrane of an eggshell consists of three layers which include inner membrane, limiting membrane surrounding the egg white shell and the outer shell. These shells are formed by ordered layers made up of 95% $CaCO_3$ (calcite) deposited on ~ 3.5% organic matrix (mainly fibrillar proteins with disulphides) cross-linked to three types of collagen (I, V and X) and glycosaminoglycans [5]. Hence, the eggshells were processed to separate the crystalline phase from these organic templates and characterized using XRD. Fig. 3a shows an X-ray diffraction pattern for theeggshell particles (micron size) with a Bragg's angle of the 100% peak at 2θº = 29.4 in the (104) crystal plane. This matched $CaCO_3$ (calcite) with JCPDS-Pdf file # 47-1743 in the data base and is also consistent with past findings on this inorganic mineral [5,13].

The amorphous silicon dioxide (15 nm) precursor was characterized as received. Fig. 3b shows the broad characteristic amorphous SiO_2 peak. This peak has an equivalent Braggs angle of 2θ = 21.8º and conforms to previous reports where 15-30 nm amorphous silica was precipitated [29]. Crystalline $CaCO_3$ is heavier than the amorphous SiO_2. In order to uniformly mix the two for reaction in a solid state without phase separations, the mixing has to be such that they can stick onto each other. Hence, the mixture of $CaCO_3$ and amorphous SiO_2were ball-milled for 100 min to form a uniform blend for the solid state reaction.

Fig. 4 presents the X-ray diffraction patterns used for monitoring the development of β-$CaSiO_3$ during the synthesis process. In this figure, diffraction pattern (a) denotes SiO_2 + $CaCO_3$ ball milled for 100 minutes. This pattern is identical to that of calcite, but also shows the amorphous

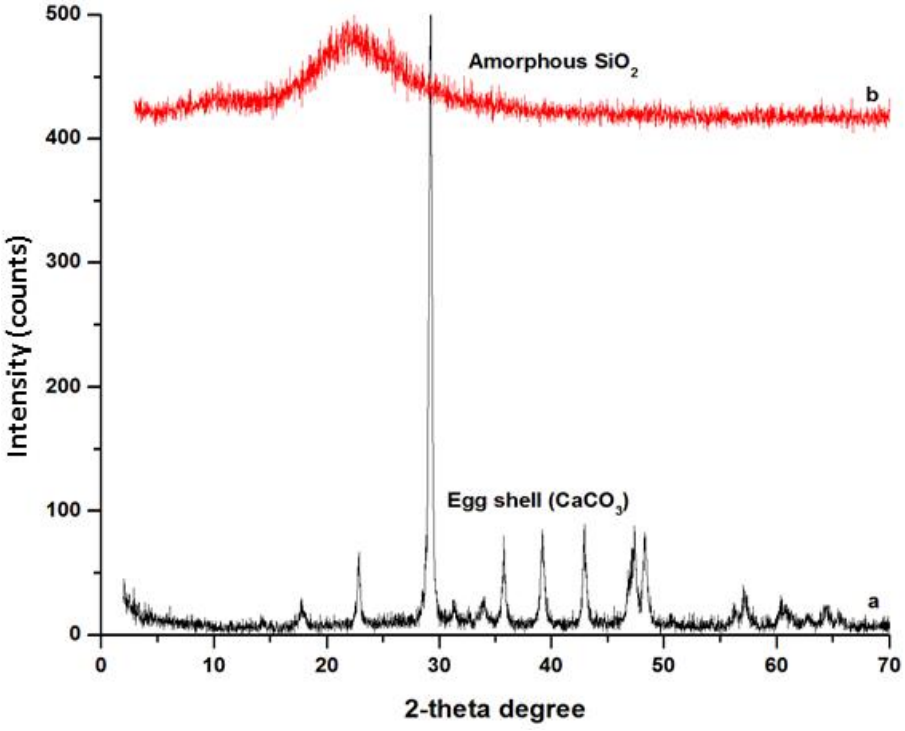

Fig. 3. X-ray diffraction patterns of the precursors: (a) eggshell, (b) silica

portion due to SiO_2 (extended region between 2θ = 15-25º with one crystal plane of $CaCO_3$ merging with it as shown in Fig. 4a This indicates that no new material was formed at this stage of the synthesis process contrasting some past report [30]. However, the use of different precursors, differences in the energy of the equipment and powder to ball ratio could be the reason for the different outcome.

The TGA residue of the material in (a) is the one in (d) which reveals a pattern analogous to that of β-$CaSiO_3$ with some imperfections. The patterns denoted b and c are for SiO_2 and $CaCO_3$ subjected to ball milling for 10 and 20 h respectively. These patterns are unique from that in (a), indicating the formation of a new material. However this could not be identified by the JCPDS database, though past reports have shown similar patterns as calcium silicate hydrates (CSH), obtained by ginding mixtures of calcium hydroxide and SiO_2 in different amounts of water [31] and another after mixing different ratios of calcium oxide and amorphous SiO_2 and aging in water for 7 days [32]. This means that our approach of ball milling for a maximum of 20 h does not yield *Wollastonite*. When the materials in a and b were sintered at 1000ºC for 3 h, the XRD pattern of the resulting materials matched *wollastonite* (β-$CaSiO_3$) as shown in the curves e and f. These curves have similar diffraction pattern as the one in d, confirming that the transitions observed in the preliminary monitoring of the reaction by TGA can be mimicked in a furnance to yield the same product. It became apparent after these series of initial experiments that if the required controlled conditions are provided, nanoscale β-$CaSiO_3$ can be synthesized using the eggshell (bio sourced $CaCO_3$) and amorphous SiO_2 precursors through these techniques. Therefore a combination of ball milling, sintering and sonochemical techniques were used to synthesis β-$CaSiO_3$ NPs. Sonochemical technique was used as an additional step to observe the effect of ultrasonic irradiation on the particle sizes and agglomerations.

3.3 Characterization of the β-$CaSiO_3$ Nano Material

Sintering causes particles of the β-$CaSiO_3$ to stick together. Hence ball milling became a necessity after sintering. β-$CaSiO_3$ NPs synthesized through a cycle of ball milling, sintering and ball milled again, is designated as BSB and those synthesized by ball milling, sintering, ball milled again followed by ultra sonication is designated as BSBU.

The sonochemical technique is imperative in the synthesis of NPs because of its success in

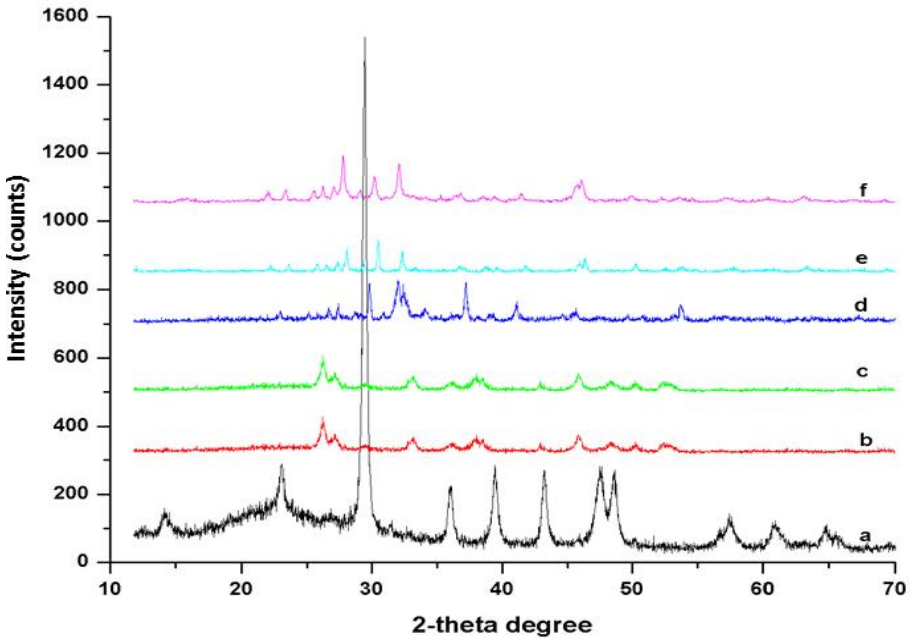

Fig. 4. X-ray diffraction analysis for monitoring the development of β-$CaSiO_3$ during synthesis: (a) precursors ball milled for 100 min, (b,c) precursors ball milled for 10 and 20 h respectively, (d) Tga residue of the material in a, (e,f) material in a and b sintered at 1000ºC respectively

minimizing particle-to-particle affinity, size reduction and morphology modification. The results of both methods are shown in the X-ray diffraction pattern in Fig. 5.

These patterns reveal prominent peak intensities at Bragg's angles, 2θº = 23.2, 25.3, 26.8, 28.9, 30.0, 32.9, 35.4, 36.2, 38.2, 39.1, 41.3, 44.7, 45.7,47.3, 48.3, 49.1, 49.7, 51.9, 53.1, 53.3, 55.2, 57.3, 59.5, 62.7, 65.0, 68.9, 74.8 and 78.8. These angles correspond to the crystal planes of standard β-$CaSiO_3$ shown in Fig. 5 in an ascending order and matched JCPDS Pdf file #98-000-0463.

The diffraction pattern of BSBU suggest that the particle sizes are smaller in this material than in BSB. This is because the peaks are broader than those of BSB. The broad nature of these peaks signifies the presence of NPs but can also be due to strain or defects in the crystalline material [17]. The narrow peaks in BSB could mean large individual particles or several agglomerates of small particles existed in the material. Particle size reduction can be associated with the random collision of the balls against the particles and the walls of the canisters several times in a second during the ball milling. Singh and Karmakar [30] reported the synthesis of $CaSiO_3$ through a solid state room temperature ball milling using $CaCO_3$ and SiO_2 in a sequential step mechanism they termed: comminution of raw materials, recombination of comminuted raw material to final product, and comminution of the final product to smaller sizes. Other reports have shown the mechanochemical synthesis of calcium silicate hydrates (CSH) and Sol-gel aging process [31,32].

The relevance of the sonochemical technique has been phenomenal, especially in the modification of inorganic materials [33]. Highly intense ultra sound irradiated liquids produce acoustic cavitation which drives bubble formation and collapse. This leads to the generation of intense and confined heating, high pressures and extreme short lifetimes capable of inducing high energy reactions [34]. The hot spots can rise to 5000ºC with about 1000 atmospheres with heating and cooling rates more than 10×10^{11} K/s. Cavity collapse close to extended solid surface trigger very fast moving jets of liquid into the surface, and creates shock wave damage to the surface [35]. The physical process responsible for the sonochemical modifications of inorganic materials are; enhancements in mass transport from chaotic mixing and acoustic streaming, generation of damages at the solid-liquid interfaces by shock wave and streams of micro jets, development of high-speed inter-particle collisions in slurries and fragmentation of brittle solid to increase surface areas [35]. Hence, further reduction in particle sizes as shown by the XRD pattern of BSBU sample was due to ultrasonic effects. Particle size of β-$CaSiO_3$ was confirmed with TEM results shown in Figs. 6a-b. They reveal the presence of irregular shaped polycrystalline β-$CaSiO_3$ with diameters less than 50 nm, supporting the XRD results.

Ball milling is simple, cheap, applicable to many types of materials and easy to scale up to large quantity production. This technique subject's materials to severe plastic deformation with compressive loads through continues impacts of the balls on them. This can produce nanosized materials with superior properties [36]. Also, the sonochemical approach is highly effective in inducing particle break down to nanoscale, dispersion of agglomerates and the production of large quantities of materials [37]. A combination of these two techniques therefore constitutes an effective method for the synthesis of β-$CaSiO_3$ NPs. The TEM results showed some particles in the range of 15-30 nm, indicating the effectiveness of the approach. This also conforms to 21 nm size particles produced in ball milling reported elsewhere [30].

The FESEM micrograph in Fig. 7 show the results for elemental analysis of the rectangular region in Fig. 7a by energy dispersive spectroscopy (EDS). This revealed the presence of only Ca, Si and O in Fig. 7b and strongly suggests that β-$CaSiO_3$ was the main material without any detectable impurities in this region.

3.4 Cytotoxic Effect of β-$CaSiO_3$

The potential toxicity of NPs has become a major concern as these particles have the ability to interact and disrupt the growth, structure and functions of organs and tissues in living organisms [18]. Toxicity has been extensively investigated and has been found to depend on physiochemical factors such as particle size, shape or morphology, surface charge and chemistry, composition, and subsequent NPs stability [18-32]. High surface area and porosity that characterized the synthesized calcium silicate nanomaterial makes it more suitable for tissue regeneration applications. In order to assess the biocompatibility of these newly synthesized materials, cytotoxicity tests in a controlled experiment based on established cell viability protocols were conducted. In this study

the effect of β-$CaSiO_3$ on the viability of human osteoblast cells (ATCC CRL 11372) was investigated. Viability assays are used to assess the overall dose-dependent toxicity of nanoparticles in cultured cells, examining cell survival and proliferation parameters after exposure to the particles [38]. Results of cytotoxicity studies presented in Fig. 8 show the status of osteoblast cells during incubation with various concentrations of β-$CaSiO_3$ NPs for 24 and 48 h. The results show that in all the tested doses of NPs, the viability of the osteoblast cells was not different from that of control cells (CM). This indicates that β-$CaSiO_3$ NPs at these concentrations do not adversely affect the physiological activities of the osteoblast cell line. In contrast, cells in the control wells treated with a cytotoxic drug, staurosporine (STS), showed a significant loss in viability, indicating the sensitivity of the cells towards cytotoxic agents.

If the NPs were toxic a dose dependent reduction of viability would be expected. These results are in agreement with past findings on *wollastonite* and other silicates in bone-bonding and soft tissue regeneration [39,40]. Also, *in vitro* evaluation of *wollastonite* and dicalcium silicate coatings seeded with osteoblast cells showed formation of apatite layers on their surfaces [41]. Also, calcium silicate hydraulic cements designed for dentistry was found to be promoting the formation of bone-like apatite, based on the composition of the culturing media and the aging time [9]. These suggest that β-$CaSiO_3$ is a good candidate for apical bone healing, particularly when it is doped with alpha-tricalcium phosphate [42]. The Ca and Si ions in β-$CaSiO_3$ play key roles in the nucleation and growth of Hydroxyapatite and have great influence on the metabolism of osteoblast cells; this is very relevant in mineralization and bone-bonding mechanism [43]. Based on the *in vitro* cell cytotoxicity study findings, β-$CaSiO_3$ show the potential as a candidate for tissue regenerating applications.

Since cytotoxicity may vary with different cell types [20,24], testing of the NPs *in vivo* are warranted to validate their potential utility for tissue engineering. The optical micrographs in Fig. 9a, candeshow the morphology of the untreated cells as they grew from day 1, 3 and 5 respectively. Panels b, d to f depicts the cells incubated with 0.1536 mg/mL concentrations of β-$CaSiO_3$ NPs from day 1 (b) to 5 (f). Both isolated and agglomerated particles attached to the cells can be observed on these micrographs (Figs. 9b to f). Themicrographs also show that no cell death occurred in the presence of the NPs by the fifth day, even in the presence of agglomerates. For instance, as depicted in Fig. 9, micrograph f taken on day 5 shows more cells per field compared to day 1 (b), suggesting that cell proliferation was not hampered. Also the cells in the first days were visible as singlets, but by the fifth day they had expanded to occupy the plate surface due to continued division. Since this trend is also visible in the control cells (a - e) we conclude that the NPs did not interfere with cell proliferation.

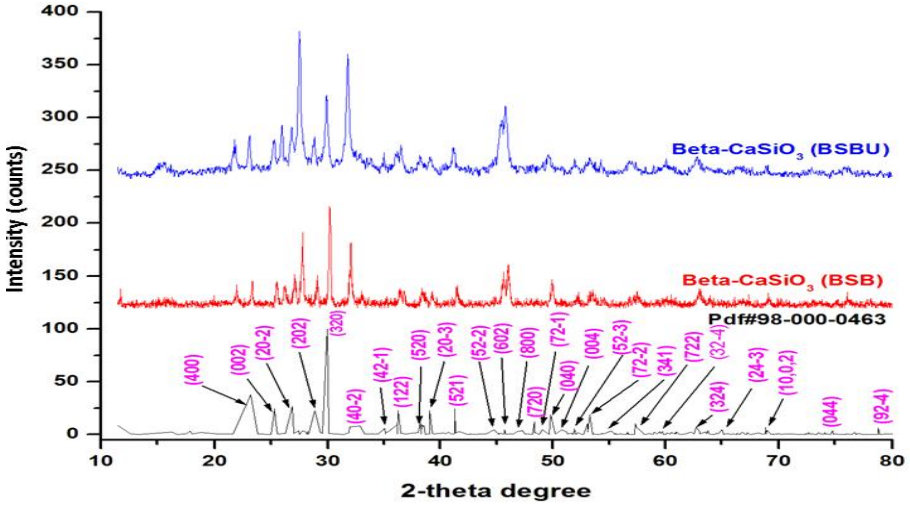

Fig. 5. X-ray diffraction patterns of β-$CaSiO_3$ subjected to two different treatments

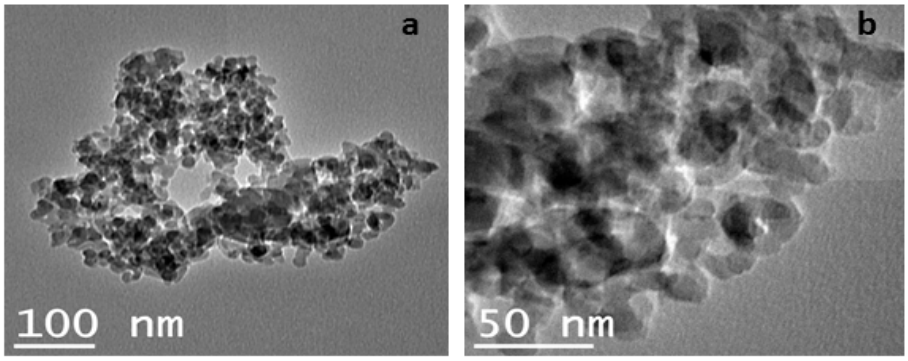

Fig. 6. TEM micrographs of the β-$CaSiO_3$ NPs; (a) low, (b) medium

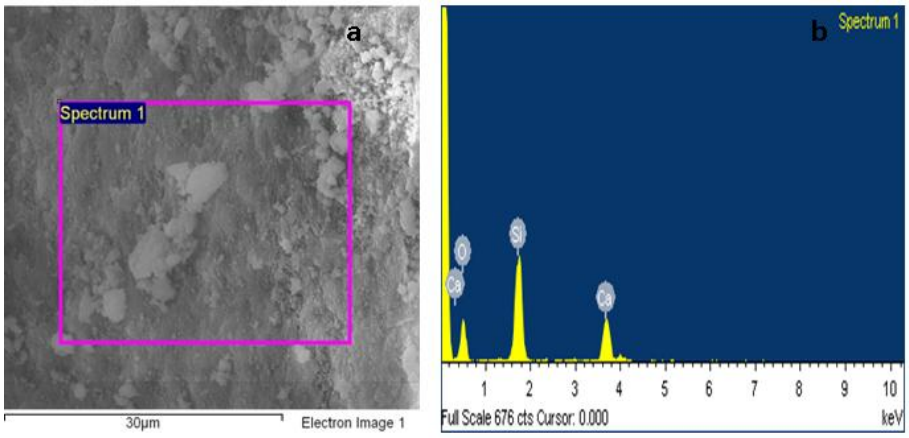

Fig. 7. Scanning electron microscope (SEM) results: (a) micrograph of β-$CaSiO_3$ NPs, (b) EDS of β-$CaSiO_3$ NPs

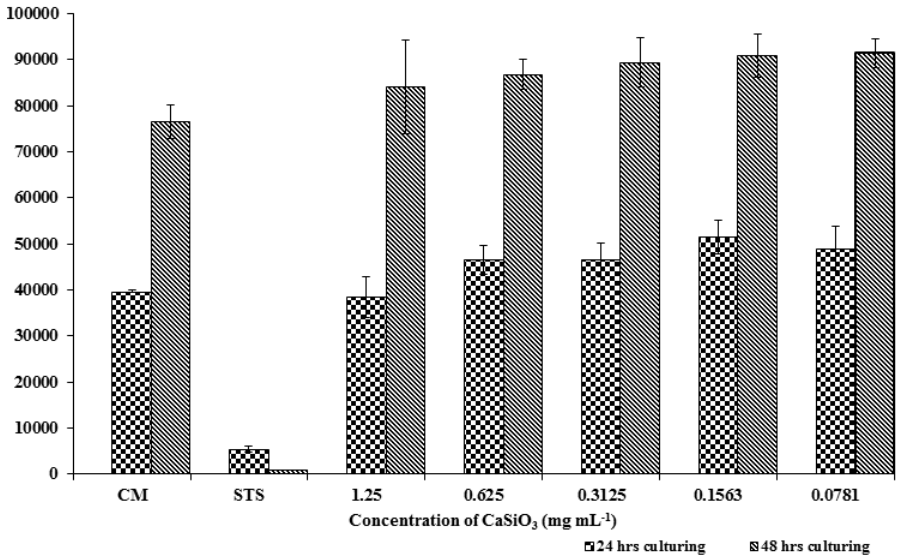

Fig. 8. Luminous intensity in CRL-1137 osteoblast cells after 24 and 48 h incubation with β-$CaSiO_3$ NPs

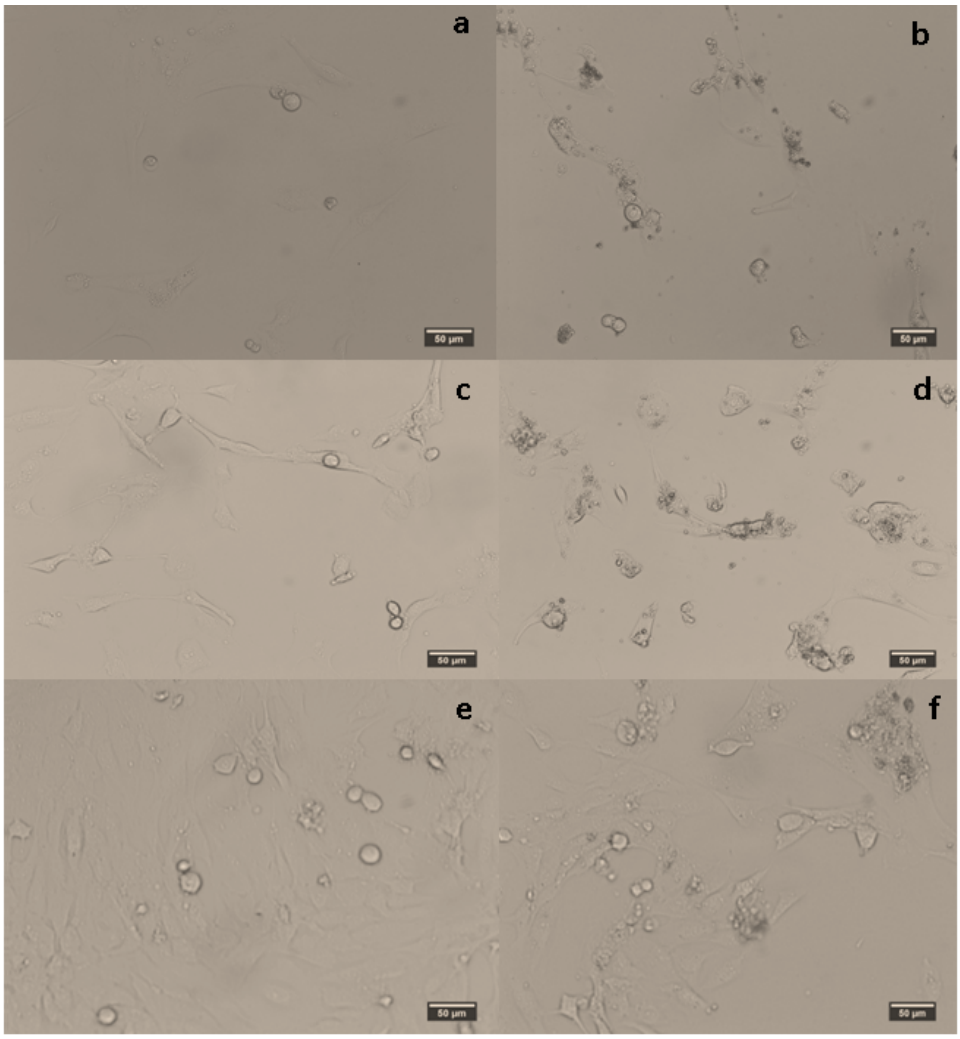

Fig. 9. Optical micrographs: (a, c, e) cultured cell only, (b, d, f) cultured cells with β-$CaSiO_3$ NPs

4. CONCLUSION

The conversion of the eggshell to β-$CaSiO_3$ through a sustainable approach was successful. $CaCO_3$ separated from eggshells was reacted with SiO_2 at high temperature. The development of β-$CaSiO_3$ during the synthesis process was monitored using FTIR, XRD and TGA. FESEM-EDS used for elemental analysis showed that the materials contain only Ca, Si and O whiles the TEM micrograph showed the particles in nanometer dimensions. The characterization showed that the use of only mechanical attrition on $CaCO_3$ and SiO_2 precursors could only produce calcium silicate hydrates (CSH). However, additional steps of sintering (3 h) re-ball milling and ultra sonication in ethanol resulted into a β-$CaSiO_3$ phase with particle sizes less than 50 nm. Cytotoxicity tests on human osteoblast cell line ATCC CRL 11372 indicated that the β-$CaSiO_3$ is biocompatible, an indication that it can used as a tissue regeneration material and other biomedical engineering applications upon further investigation. This is essentially a conversion of bio waste into a useful bio material. Such findings are promising and suggest that the natural and more environmentally benign eggshells can substitute toxic precursors in the synthesis of multifunctional β-$CaSiO_3$ and others like calcium silicate hydrates with the use of sustainable techniques, instead of discarding it in the already waste populated landfills.

ACKNOWLEDGEMENTS

The financial support of the NSF-CREST#1137681, NSF-RISE#1137682 Alabama EPSCoR #1158862 and The Alabama Commission on Higher Education is gratefully acknowledged. Research in T.S. laboratory is supported by NIH grants U54CA118948, SC3GM109314 and G12MD007585 and we are also grateful for all the assistance in cytotoxicity analysis. Our gratitude also goes to American Dehydrated Foods, Inc., Atlanta GA, USA, for the free provision of the eggshells. Funding agencies did not take part in the design, collection, analysis and interpretation of the data.

COMPETING INTERESTS

Authors have declared that no competing interests exist.

REFERENCES

1. Walton HV, Cotteril OJ, Vandepop JM. Composition of shell waste from egg breaking plants. Poult. Sci. 1973;52(5): 1836-41.
2. Adams RG, Franklin MR. Vacuum treatment of an input stream without ruining delicate output fractions. US Pat. 7017 277 B1; 2006.
3. Felipe-Sese M, Eliche-Quesada D, Corpas-Iglesias FA. The use of solid residues derived from different industrial activities to obtain calcium silicates for use as insulating construction materials. Ceram. Int. 2011;37(8):3019-28.
4. Dodson RJ, Hunt JA, Parker LH, Yang Y, Clark HJ. Elemental sustainability: Towards the total recovery of scarce metals. Chem. Eng. Process. 2012;51:69-78.
5. Nys Y, Gautron J, Garcia-Ruiz JM, Hincke MT. Avian eggshell mineralization biochemical and functional characterization of matrix proteins.CR Palevol. 2004;3(6-7): 549-56.
6. Lin K, Chang J, Liu Z, Zeng Y, Shen R. Fabrication and characterization of 45S5 bioglass reinforced macroporous calcium silicate bioceramics. J. Eur. Ceram. Soc. 2009;29(14):2937-43.
7. Hench LL, Polak JM. Third-generation biomedical materials. Science. 2002; 295(5557):1014-17.
8. Gandolfi MG, Farascioni S, Pashley DH, Gasparotto G, Prati C. Calcium silicate coating derived from portland cement as treatment for hypersensitive dentine. J. Dent. 2008;36(8):565-78.
9. Gandolfi MG, Ciapetti G, Taddei P, Perut F, Tinti A, Cardoso MV, et al. Apatite formation on bioactive calcium-silicate cements for dentistry affects surface topography and human marrow stromal cells proliferation. Dent. Mater. 2010; 26(10):974-92.
10. Thompson SP, Day SJ, Parker JE, Evans A, Tang CC. Fine-grained amorphous calcium silicate $CaSiO_3$ from vacuum dried sol-gel-production, characterization and thermal behavior. J. Non-Cryst. Solids. 2012;358(5):885-92.
11. Kaili L, Wanyin Z, Siyu N, Jiang C, Yi Z, Weijun Q. Study of mechanical property and *In vitro* biocompatibility of $CaSiO_3$ ceramics. Ceram. Int. 2005;31(2):323-26.
12. Siyu N, Jiang C, Lee C, Wanyin Z. Comparison of osteoblast-like cell response to calcium silicate and tricalcium phosphate ceramic *In vitro*. J. Biomed. Mater. Res. Part B: Appl. Biomater. 2007; 80B(1):174-83.
13. Nuchnapa T, Tunchanoke K, Supawinee K, Ruksapong K, Anuvat S. An innovative $CaSiO_3$ dielectric material from eggshells by sol-gel process. J. Sol-Gel. Sci. Technol. 2011;58(1):33-41.
14. Julio AC, Alvaro A. Ecological and toxicological effects of inorganic nitrogen pollution in aquatic ecosystems: A global assessment. Envron. Int. 2006;32(6):831-49.
15. Juan CA, Rodney A, Klaus SL, Francis M, Edward R, Juan CS, Katsunori Y, Ron Z. Mineral carbonation and industrial uses of carbon dioxide. In: Bert M, Ogunlade D, Heleen de C, Manuela L, Leo L. (Eds.). Carbon dioxide capture and storage. United Kingdom: Cambridge University Press; 2005.
16. Zhang L, Webster JT. Nanotechnology and nanomaterials: Promises for improved tissue regeneration. Nano Today. 2009; 4(1):66-80.
17. Li X, Wang L, Fan Y, Feng Q, Cui FZ. Biocompatibility and toxicity of nanoparticles and nanotubes. J. Nanomater. 2012;19.
DOI:10.1155/2012/548389.

18. Buzea C, Blandino PII, Robbie K. Nanomaterials and nanoparticles: Sources and toxicity. Biointerphases. 2007;2(4):17-172.
19. Kong B, Seog HJ, Graham LM, Lee BS. Experimental considerations on the cytotoxicity of nanoparticles. Nanomedicine-UK. 2011;6(5):929-41.
20. Shinde SK, Grampurohit ND, Gaikwad DD, Jadhav L, Gadhave MV, Shelke PK. Toxicity induce by nanoparticles. Asian Pac. J. Trop. Dis. 2012;2(4):331-34.
21. Ai J, Biazar E, Jafarpour M, Montazeri M, Majdi A, Aminifard S, et al. Nanotoxicology and nanoparticle safety in biomedical designs. Int. J. Nanomed. 2011;6:1117-27.
22. Sohaebuddin KS, Thevenot TS, Baker D, Eaton WJ, Tang L. Nanomaterial cytotoxicity is composition, size, and cell type dependent. Part. Fibre Toxicol. 2010;7:22. DOI: 10.1186/1743-8977-7-22.
23. Webster JT. Nanomedicine: Real commercial potential or just hype? Int. J. Nanomed. 2006;1(4):373-374.
24. Alkilany MA, Catherine J, Murphy JM. Toxicity and cellular uptake of gold nanoparticles: what we have learned so far? J. Nanopart. Res. 2010;12(7):2313-33.
25. Wang L, Nagesha KD, Selvarasah S, Dokmeci RM, Carrier LR. Toxicity of CdSe Nanoparticles in Caco-2 Cell Cultures. J. Nanobiotechnology. 2008;6:11.
    DOI:10.1186/1477-3155-6-11.
26. Meiszterics A, Sinko K. Sol-gel drived calcium silicate ceramics. Colloid Surfaces A. 2008;319(1-3):143-48.
27. Saravanapavan P, Hench LL. Mesoporous calcium silicate glasses I. Synthesis. J. Non-Cryst. Solids. 2003;318(1):1-13.
28. Saito F, Mi G, Hanada M. Mechanochemical synthesis of hydrated calcium silicates by room temperature grinding. Solid State Ionics. 1997;101-103(1):37-43.
29. Musić S, Filipović-Vinceković N, Sekovanić L. Precipitation of amorphous SiO_2 particles and their properties. Braz. J. Chem. Eng. 2001;28(4):89-94.
30. Singh SP, Karmakar B. Mechanochemical synthesis of nano calcium silicate particles at room temperature. New J. Glass Ceram. 2011;1(2):49-52.
31. Sugiyama D. Chemical alteration of calcium silicate hydrate (C-S-H) in sodium chloride solution. Cement and Concrete Res. 2008;38(11):1270-75.
32. Rangari KV, Mohammad MG, Jeelani S, Butenko VY, Dhanak RV. Synthesis and characterization of diamond-coated CNTs and their reinforcement in nylon-6 single fiber. ACS. Appl. Mater. Inter. 2010;2(7): 1829-34.
33. Suslick KA. Sonochemistry of transition metal compounds. In: King BR. (Eds.), Encyclopedia of inorganic chemistry. New York: J. Wiley & Sons. 1994;7.
34. Suslick KS, Crum LA. Sonochemistry and Sonoluminescence, In: Crocker MJ. (Eds.), Encyclopedia of Acoustics. New York:Wiley-Interscience. 1997;1.
35. Suslick KS, Fang MM, Hyeon T, Mdleleni MM. Applications of sonochemistry to materials synthesis. In: Sonochemistry and sonoluminescence. Crum LA, Mason TJ, Reiss J, Suslick KS. (Eds.). Netherlands; Kluwer Publishers; 1999.
36. Rao BJ, Catherin JG, Murthy NI, Rao VD, Raju NB. Production of nano structured silicon carbide by high energy ball milling. Int. J. Eng. Sci. Technol. 2011;3(4):82-88.
37. Saravanan P, Gopalan R., Chandrasekaran V. Synthesis and characterization of nanomaterials. Defence Sci. J. 2008;58(4):504-16.
38. Sprio S, Tampieri A, Celotti G, Landi E. Development of hydroxyapatite/calcium silicate composites addressed the design of load-bearing bone scaffolds. J. Mech. Behav. Biomed. Mater. 2009;2(2):147-55.
39. Fujiwura M, Shiokawa K, Kubota T. Direct encapsulation of proteins into calcium silicate by water / oil / water interfacial reaction method and their responsive release behaviors. Mater. Sci. Eng. C. 2012;32(8):2484-90.
40. Liu X, Ding C, Chu KP. Comparison of in-vitro evaluation of wollastonite and dicalcium silicate coating. Key Eng. Mater. 2005;288-289:359-62.
41. Gandolfi GM, Taddei P, Tinti A, Dorigo SDE, Prati C. Alpha-TCP improves the apatite-formation ability of calcium-silicate hydraulic cement soaked in phosphate solutions. Mater. Sci. Eng. C. 2011;31: 1412-22.

42. Wu C, Chang J, Wang J, Ni SE, Zhai W. Preparation and characteristics of a calcium magnesium silicate (bredigite) bioactive ceramic. Biomaterials. 2005; 26(16):2925-31.

43. Christenson EM, Anseth KS. van den Beucken JJ, Chan CK, Ercan B, Jansen J A, et al. Nanobiomaterial Applications in Orthopedics. J. Orthopaed. Res. 2007; 25(1):11-22.

Peer-review history:
The peer review history for this paper can be accessed here:
http://www.sciencedomain.org/review-history.php?iid=1070&id=5&aid=8601